M. Jouili
K. Jarray
Y. Koubaa
M. Boussak

J. Electrical Systems 8-1 (2012): 108-118

Regular paper

Implementation of Sensorless Speed Control for Induction Motor drive Using IRFOC

The aim of this paper is to implement a sensorless indirect rotor-flux-oriented control (IRFOC) of induction motor (IM) drives. Indeed, the proposed method for speed estimation is based on Luenberger state observer (LSO). The adaptive rotor speed is actually derived from Lyapunov stability theory by using measured and estimated stator currents and estimated rotor flux. The proposed control scheme, as a result, achieves a good performance with computational complexity reduction obtained by using the analytical relation to determine the LSO gain matrix. Again, the observer is simple and robust, when compared with the previously developed observers, and suitable for online implementation. The design, analysis, and implementation for a 3-kW induction motor are completely carried out using a dSpace DS 1104 digital signal processor (DSP) based real-time data acquisition control (DAC) system, and MATLAB/Simulink environment. Digital simulation and experimental results are presented to show the improvement in performance of the proposed algorithm.

Keywords: Rotor flux orientation, feed-forward decoupling, induction motor drive, sensorless vector control, Luenberger state observer (LSO).

1. INTRODUCTION

Due to their high performances in terms of reliability, robustness and efficiency, the adjustable ac-motor drives are increasingly adopted in most industrial applications such as military, aerospace and automotive industries [1]. The aforementioned qualities have been researched and improved by using intelligent and sophisticated control methods based on the field oriented control (FOC) because it controls both the amplitude and phase of ac-excitations. The vector control technique has been widely used for high-performance induction motor drives, where the knowledge of the rotor speed is necessary. This information is provided by an incremental encoder, which is the most common positioning transducer used today in industrial applications [2, 3]. The use of this sensor, nevertheless, implies more electronics, higher cost, lower reliability, and difficulty in mounting in some cases such as motor drives in harsh environment and high speed drives, increase in weight, increase in size, and increase in electrical susceptibility.

To overcome these problems, in recent years, the elimination of the transducers has been considered as an attractive prospect. Therefore, numerous approaches have been proposed to estimate rotor velocity and/or position.

In recent literature, many researchers have carried out the design of sensorless vector control induction motor drives. These methods, definitely, are based on the following schemes:

- Model Reference Adaptive System (MRAS) [4-7];
- Extended Kalman Filter (EKF) [8-9];
- Luenberger observer [10-14];
- Artificial neural network [15-17]

Indeed, some of these methods require specially modified machines and the injection of

Corresponding author : yassine.koubaa@enis.rnu.tn
Research Unit of Automatic Control (UCA), University of Sfax, National Engineering School of Sfax (ENIS), B.P. 1173 Sfax, Tunisia.

Copyright © JES 2012 on-line : journal/esrgroups.org/jes

disturbance signals or the use of a machine model. Otherwise, all other methods for speed estimation using a machine model fed by stator quantities are parameter dependent; therefore, parameter errors can degrade the speed control performance. Thus, some kind of parameter adaptation is required in order to obtain high-performance sensorless vector control drive.

In this paper, a sensorless indirect rotor-flux-oriented control (IRFOC) of induction motor drives is studied. The rotor speed is estimated by the designed-observer by relying on the measured and estimated stator currents and estimated rotor fluxes. As a matter of fact, this observer is designed to simultaneously estimate the rotor speed, the rotor flux and stator currents. The singular perturbation theory is used to get a sequential and simple design of the observer, and the flux observer stability is ensured through the Lyapunov theory. Afterwards, a full description and justification of the proposed algorithm is given and its performances are tested by simulations and experiments. Although related algorithms have previously been presented, the following contributions are believed to be new. First, the dynamic and steady-state performances are analyzed. Excellent behaviour is verified in most cases. Second, the use of the rotor flux oriented control and a general framework is developed.

As a whole, this paper is organized as follows: in Section 2, we briefly review the indirect rotor-flux-oriented control (IRFOC) of induction motor (IM) drives. The feedforward decoupling controller is described in Section 3. In Section 4, the sensorless speed control algorithm is presented. Experimental and simulation results are presented in Section 5. Finally, conclusions and comments are summarized in Section 6.

2. ROTOR ORIENTATION STRATEGY

For IRFOC, the rotor flux vector is aligned with d-axis and setting the rotor flux to be constant equal to the rated flux, which means $\Phi_{dr} = \Phi_r$ and $\Phi_{qr} = 0$.

The dynamic model of an induction motor car be represented according to the usual d-q axis components is asynchronous rotating frame as

$$v_{ds} = \sigma L_s \left(p + \frac{1}{\sigma\tau_s} + \frac{1-\sigma}{\sigma\tau_r} \right) i_{ds} - \sigma L_s \omega_s i_{qs} - \frac{M}{L_r \tau_r} \Phi_r \tag{1}$$

$$v_{qs} = \sigma L_s \left(p + \frac{1}{\sigma\tau_s} + \frac{1-\sigma}{\sigma\tau_r} \right) i_{qs} + \sigma L_s \omega_s i_{ds} + \frac{M}{L_r} \omega_r \Phi_r \tag{2}$$

$$\Phi_r = \frac{M}{1+\tau_r p} i_{ds} \tag{3}$$

$$T_e = n_p \frac{M}{L_r} i_{qs} \Phi_r \tag{4}$$

$$\omega_{sl} = \frac{M}{\tau_r \Phi_r} i_{qs} \tag{5}$$

Where $\omega_{sl} = \omega_s - \omega_r$, $\tau_s = \frac{L_s}{R_s}$, $\tau_r = \frac{L_r}{R_r}$ and $\sigma = 1 - \frac{M^2}{L_s L_r}$

It can be seen that is the rotor flux is kept constant; the torque can be controlled by controlling the q-axis current.

The electromagnetic torque equation and the electrical angular speed motor are related by

$$J\frac{d\omega_r}{dt}+f\omega_r=n_p\left(T_e-T_l\right) \tag{6}$$

3. FEEDFORWARD DECOUPLING CONTROLLER

It can be seen that the d-axis and q-axis voltage equations are coupled by the terms $-\sigma L_s\omega_s i_{qs}-\frac{M}{L_r\tau_r}\Phi_r$ and $\sigma L_s\omega_s i_{ds}+\frac{M}{L_r}\omega_r\Phi_r$. These terms are considered as disturbances are and cancelled by using a decoupling method that utilizes non linear feedback of the coupling voltages. If the decoupling method is implemented the voltage equations become [18].

$$v_d=v_{ds}+E_d=\sigma L_s\left(p+\frac{1}{\sigma\tau_s}+\frac{1-\sigma}{\sigma\tau_r}\right)i_{ds} \tag{7}$$

$$v_q=v_{qs}+E_q=\sigma L_s\left(p+\frac{1}{\sigma\tau_s}+\frac{1-\sigma}{\sigma\tau_r}\right)i_{qs} \tag{8}$$

Where $E_d=\sigma L_s\omega_s i_{qs}+\frac{M}{L_r\tau_r}\Phi_r$ and $E_q=-\sigma L_s\omega_s i_{ds}-\frac{M}{L_r}\omega_r\Phi_r$; E_d and E_q are, respectively the d-axis and q-back electromotive force (EMF).

Thus, the dynamics of the d-axis and q-axis currents are now represented by simple linear first-order differential equations. Therefore, it is possible to effectively control the currents with a PI controller.

In Fig. 1, k_{ii} and k_{ip} denote proportional and integral gains of the PI d, q axis current controller, respectively. $G_d(p)$, $G_q(p)$ are the no decoupling electrical d, q axis transfer functions of the induction machine. It should be noted that the estimated values, denoted by ^, are introduced to cancel out the coupling terms in the induction motor model.

If we assume that the back EMFs are canceled by the feedforward compensation term, we obtain

$$G_d(p)=G_q(p)=\frac{K_c}{1+\tau_c p} \tag{9}$$

Where $K_c=\frac{\tau_r}{R_s\left(\tau_s+\tau_r\right)}$ is a gain and $\tau_c=\frac{\sigma\tau_r\tau_s}{\tau_s+\tau_r}$ is a time constant.

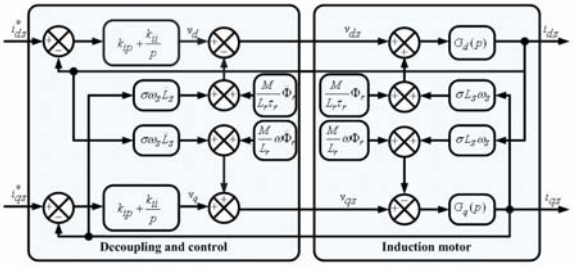


Figure 1: Block diagram of the conventional PI controller with feed forward decoupling method

The closed-loop current transfer function is

$$\frac{i_{ds}}{i_{ds}^*} = \frac{i_{ds}}{i_{ds}^*} = \frac{\omega_n^2}{p^2 + 2\xi\omega_n + \omega_n^2}\left(1 + \frac{k_{ip}}{k_{ii}}p\right) \tag{10}$$

Where $\omega_n = \sqrt{\frac{K_c k_{ii}}{\tau_c}}$ and $\xi = \frac{1 + K_c + k_{ip}}{2\omega_n \tau_c}$ and ω_n and ξ denote natural frequency and damping ratio, respectively. When the dynamics of the d- and q-axes currents are equivalent, the PI gains can be copied to the q-axis controller.

4. SENSORLESS SPEED CONTROL ALGORITHM

The state model of the induction motor can be described in a rotating reference frame by:

$$\begin{cases} \dot{x}(t) = Ax(t) + Bu(t) \\ y(t) = Cx(t) \end{cases} \tag{11}$$

The Luenberger state observer for estimating the stator current and the rotor flux, using the measured stator currents and voltages, is described by the following set of equations [14]:

$$\begin{cases} \dot{\hat{x}}(t) = \left(\hat{A} - LC\right)\hat{x}(t) + Bu(t) + Ly(t) \\ \hat{y}(t) = C\hat{x}(t) \end{cases} \tag{12}$$

Where $x = \begin{bmatrix} i_{ds} & i_{qs} & \Phi_{dr} & \Phi_{qr} \end{bmatrix}^T$; $\hat{x} = \begin{bmatrix} \hat{i}_{ds} & \hat{i}_{qs} & \hat{\Phi}_{dr} & \hat{\Phi}_{qr} \end{bmatrix}^T$;

$y = \begin{bmatrix} i_{ds} & i_{qs} \end{bmatrix}^T$; $\hat{y} = \begin{bmatrix} \hat{i}_{ds} & \hat{i}_{qs} \end{bmatrix}^T$; $u = \begin{bmatrix} v_{ds} & v_{qs} \end{bmatrix}^T$

$$A = \begin{bmatrix} -\gamma I_2 & \delta\left(\frac{1}{\tau_r} I_2 - \omega_r J\right) \\ \frac{M}{\tau_r} I_2 & -\left(\frac{1}{\tau_r} I_2 - \omega_r J\right) \end{bmatrix}; \quad \hat{A} = \begin{bmatrix} -\gamma I_2 & \delta\left(\frac{1}{\tau_r} I_2 - \hat{\omega}_r J\right) \\ \frac{M}{\tau_r} I_2 & -\left(\frac{1}{\tau_r} I_2 - \hat{\omega}_r J\right) \end{bmatrix};$$

$C = \begin{bmatrix} I_2 & 0_2 \end{bmatrix}$; $I_2 = \begin{bmatrix} 1 & 0 \\ 0 & 1 \end{bmatrix}$; $J = \begin{bmatrix} 0 & -1 \\ 1 & 0 \end{bmatrix}$; $0_2 = \begin{bmatrix} 0 & 0 \\ 0 & 0 \end{bmatrix}$

$\gamma = \frac{1}{\sigma L_s}\left(R_s + \frac{M^2}{\tau_r L_r}\right)$ and $\delta = \frac{M}{\sigma L_s L_r}$

Where ^ denotes the estimated values, $\hat{x}(t)$ is the observer state vector and L is the observer gain matrix, which is selected so that the system will be stable.

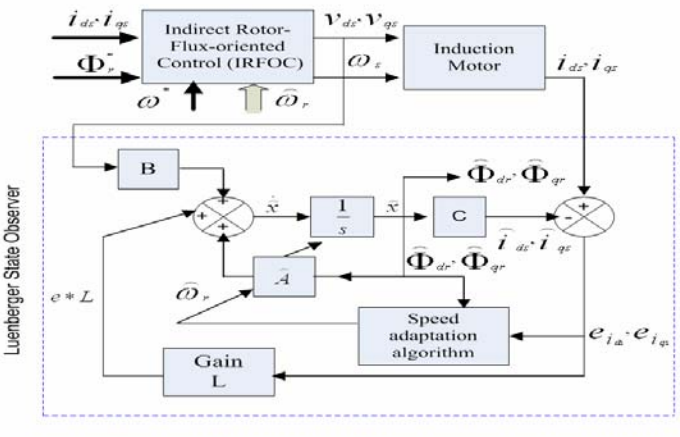


Figure 2: Speed adaptive flux observer

To ensure that the estimation error vanishes over time for any, $\tilde{x}(0)$ we should select the observer gain matrix *L* so that *(A-LC)* is asymptotically stable. Therefore, the observer gain matrix should be chosen so that all eigenvalues of *(A-LC)* have negative real parts.

To ensure stability for all range speed, the conventional procedure is to select the observer poles proportional to the motor poles (the proportionality constant is $k_p \succ 1$). If the poles of the induction motor are given by λ_{IM}, the observer poles λ_{LO} are selected as:

$$\lambda_{LO} = k_p \lambda_{IM} \tag{13}$$

This can be achieved by defining the observer matrix L in a special form

$$L = \begin{bmatrix} l_1 I_2 + l_2 J \\ l_3 I_2 + l_4 J \end{bmatrix} = \begin{bmatrix} L_1 \\ L_2 \end{bmatrix} \tag{14}$$

To determine the eigenvalues of the matrix A, we use

$$\det\left(\lambda_{IM} I_4 - A\right) = \begin{vmatrix} \lambda_{IM} + \gamma I_2 & -\delta\left(\frac{1}{\tau_r} I_2 - \omega_r J\right) \\ -\frac{M}{\tau_r} I_2 & \lambda_{IM} + \left(\frac{1}{\tau_r} I_2 - \omega_r J\right) \end{vmatrix} = 0 \tag{15}$$

In order to simplify the equation we define

$$a = \gamma I_2 \,;\; b = \frac{1}{\tau_r} I_2 - \omega_r J \;\text{ and }\; a = \frac{M}{\tau_r} I_2$$

The characteristic equation of the matrix *A* is then

$$\lambda_{IM}^2 + (a+b)\lambda_{IM} + (a - \delta c) b = 0 \tag{16}$$

To determine the eigenvalues of the matrix *(A-LC)*

$$\det\left(\lambda_{LO} I_4 - (A - LC)\right) = \begin{vmatrix} \lambda_{LO} + \gamma I_2 + L_1 & -\delta\left(\frac{1}{\tau_r} I_2 - \omega_r J\right) \\ -\frac{M}{\tau_r} I_2 + L2 & \lambda_{LO} + \left(\frac{1}{\tau_r} I_2 - \omega_r J\right) \end{vmatrix} = 0 \tag{17}$$

Hence, the characteristic equation is

$$\lambda_{LO}^2 + \left(L_1 + a + b\right)\lambda_{LO} + \left(\left(a - \delta c\right) - \left(L_1 + \delta L_2\right)\right)b = 0 \tag{18}$$

Substituting (13) in (18) gives

$$k_p^2\lambda_{IM}^2 + k_p\left(L_1 + a + b\right)\lambda_{IM} + \left(\left(a - \delta c\right) - \left(L_1 + \delta L_2\right)\right)b = 0 \tag{19}$$

The identification of (19) and k_p^2 ∗(16) gives the following results:

$$\begin{cases} l_1 = \left(k_p - 1\right)\left(\gamma + \dfrac{1}{\tau_r}\right) \\ l_2 = \left(k_p - 1\right)\hat{\omega}_r \\ l_3 = \dfrac{\left(k_p^2 - 1\right)}{\delta}\left(\gamma - \delta\dfrac{M}{\tau_r}\right) + \dfrac{\left(k_p - 1\right)}{\delta}\left(\gamma + \dfrac{1}{\tau_r}\right) \\ l_4 = \dfrac{\left(k_p - 1\right)}{\delta}\hat{\omega}_r \end{cases} \tag{20}$$

When the motor speed is not measured, it is treated as an unknown parameter in the observer (13). By adding an adaptive scheme for estimating the rotor speed to the observer, both states and unknown parameters can be estimated simultaneously. The adaptive scheme is derived by using the Lyapunov theory.

From (12) and (13), the estimation error of the stator current and the rotor flux is given by the following equation:

$$\dot{e} = \left(A + LC\right)e + \Delta A\hat{x} \tag{21}$$

Where $e = x - \hat{x}$; $\Delta A = A - \hat{A} = \begin{bmatrix} 0 & -\dfrac{1}{\sigma L_s}\Delta\omega_r J \\ 0 & J\Delta\omega_r \end{bmatrix}$ and $\Delta\omega_r = \omega_r - \hat{\omega}_r$

We define a Lyapunov function candidate V

$$V = e_n^2 e_n + \frac{\left(\Delta\omega_r\right)^2}{\lambda} \tag{22}$$

Where λ is a positive constant and $e_n = \begin{bmatrix} i_s - \hat{i}_s & \Phi_r - \hat{\Phi}_r \end{bmatrix} = \Gamma e$

With Γ a non-singular matrix

For the derivation of the adaptive mechanism, the unknown parameter $\hat{\omega}_r$ is considered constant. The time derivative of V becomes

$$\dot{V} = e_n^T \left\{ \left[\Gamma \left(A + LC \right) \Gamma^{-1} \right]^T + \left[\Gamma \left(A + LC \right) \Gamma^{-1} \right] \right\} e_n + \tilde{x}^T \Gamma \Delta A^T e_n + e_n^T \Gamma \Delta A \tilde{x} - 2\Delta\omega_r \frac{d}{dt} \frac{\left(\Delta\omega_r \right)}{\lambda} \quad (23)$$

The adaptive scheme for speed estimation is given by:

$$\hat{\omega}_r = k_{P\hat{\omega}_r} \left(e_{i_{ds}} \Phi_{qr} - e_{i_{qs}} \Phi_{dr} \right) + k_{I\hat{\omega}_r} \int \left(e_{i_{ds}} \Phi_{qr} - e_{i_{qs}} \Phi_{dr} \right) dt \quad 24)$$

5. SIMULATION AND EXPERIMENTAL RESULTS

To implement the proposed sensorless IRFOC of induction motor drive, an experimental testing ground was carried out. It' is essentially composed of:

- A squirrel-cage IM a 3Kw whose parameters are listed in appendix.
- A static power electronics convertor from semikron composed of a diode rectifier and a three-leg voltage source IGBT inverter.
- Current sensors of Hall.
- A dSpace DS 1104 ACE Kit with control desk software plugged in a Pentuim 4 personnel computer.

For implementation of the proposed sensorless IRFOC of induction motor drive, an experimental has been carried out (Fig. 4). The sensorless IRFOC algorithm is programmed with Matlab-Simulink and downloaded in the dSpace 1104 control board, offering a four-channel 16-bit (multiplexed) ADC and four 12-bit ADC units. A sampling period of 50µs is selected and the insulated gate bipolar transistors (IGBTs) are working at a switching frequency of 10 kHz with a dead time of 20µs. The load is generated through a magnetic powder brake coupled to the induction motor. The output control signals of the Slave I/O PWM are of TTL level 5V, whereas IGBTs of the static inverter must receive signals of 15V. An adaptation interface board using the integrated circuit IR2130 from International rectifier is realized.

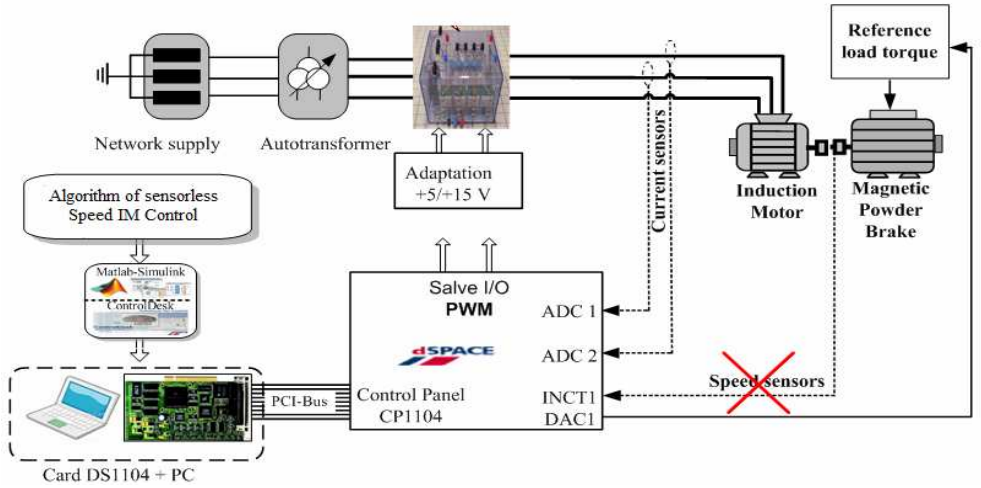
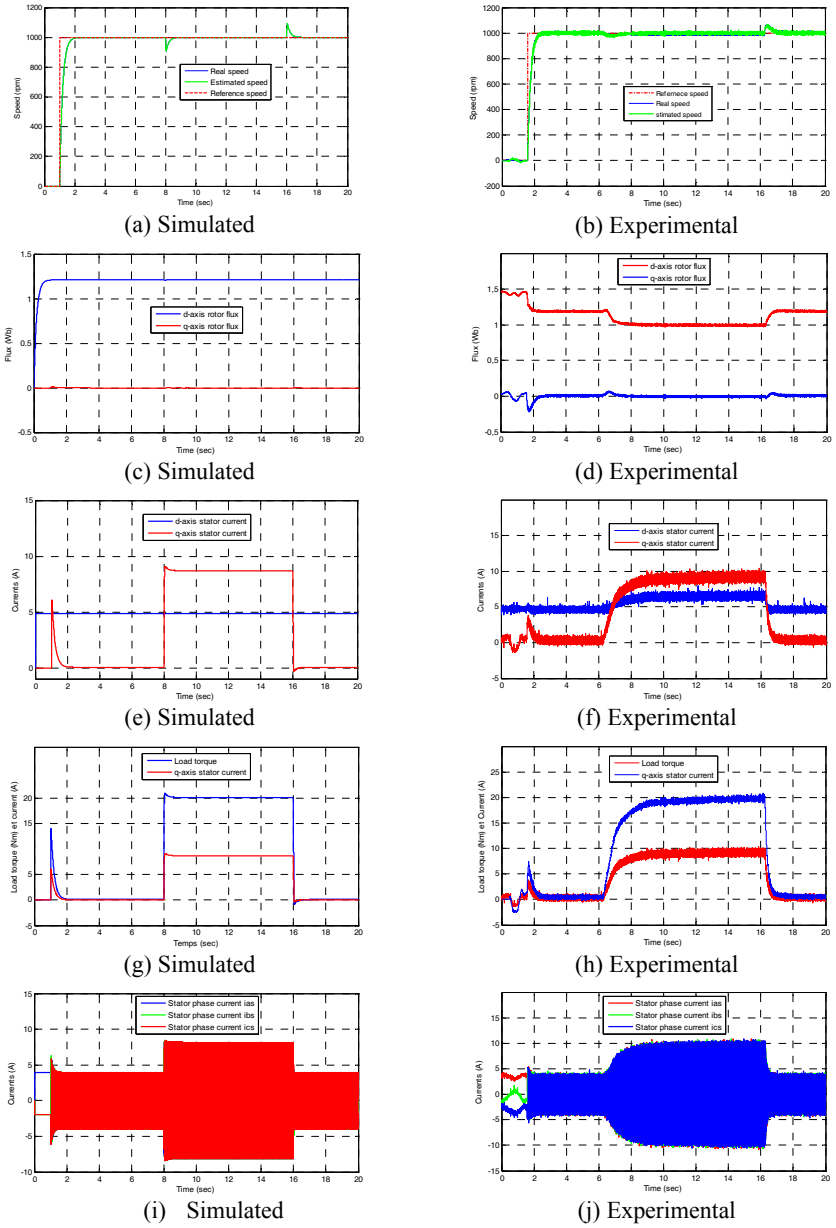


Figure 4: Scheme used for experimental setup

The simulation and experimental results obtained with the proposed IRFOC control strategy are shown in Figs. 5 and 6. Here, the reference flux is kept constant at the nominal value 1.21 Wb.

As a first test some simulation and experimental results for sensorless speed control are presented in Fig. 5 for 1000 rpm speed reference command and load torque of 20 Nm

applied and removed at t = 8 and 16 s respectively.



(a) Simulated (b) Experimental

(c) Simulated (d) Experimental

(e) Simulated (f) Experimental

(g) Simulated (h) Experimental

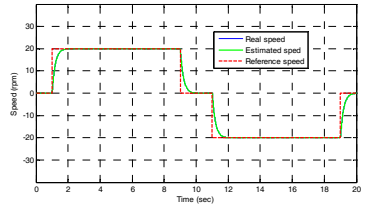
(i) Simulated (j) Experimental

Figure 5: Simulation and experimental results of step response $\omega^* = 1000$ rpm with load torque applied at 8s

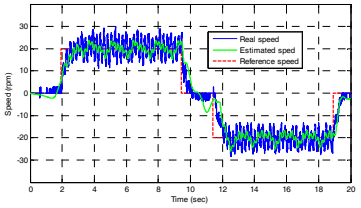
Figs. 5(a) and (b), simulation and experimental results of the reference, real and estimated rotor speed are shown. The simulation and experimental results presented in Figs. 5(c) and (d) show that the rotor fluxes converge from their initial values for their final values, respectively ($\Phi_{dr} = \Phi_r$ and $\Phi_{qr} = 0$). In Figs. 5(e) and (f), simulation and experimental results of d-q axis currents are presented. Figs. 5(g) and (h) show, respectively, simulation results and measurement of load torque and q-axis stator current.

One may also note in Figs. 5(g) and (h) that the q-axis current i_{qs} is the same shape as the electromagnetic torque. Furthermore, simulation results and measured stator phase currents are given in Figs. 5(i) and (j).

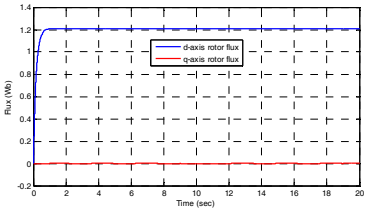
As second test, Fig. 6 shows the rotor speed control performance in the low-speed operation region (20 rpm) of the rotor speed sensorless drive. In Figs. 6(c) and (d), simulation and estimated results of d-q axis rotor flux are presented.



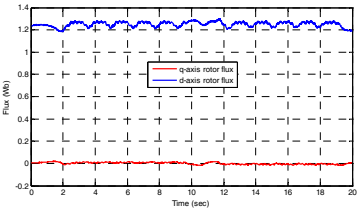
(a) Simulated



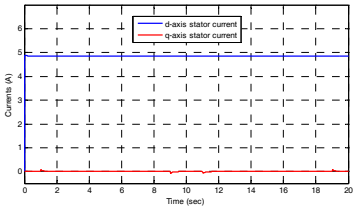
(b) Experimental



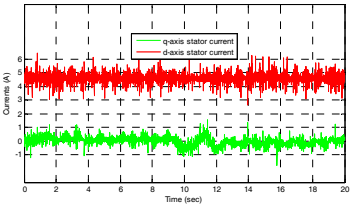
(c) Simulated



(d) Experimental



(e) Simulated



(f) Experimental

Figure 6: Simulation and experimental results for reversing speed reference from $\omega^* = 20$ rpm to $\omega^* = -20$ rpm

Besides, simulation and measured results for d-q axis currents are given in Figs. 6(e) and (f). It is shown that the proposed algorithm has good speed estimation and adequate vector control characteristics at low rotor speed operation.

5. CONCLUSIONS

In this paper, we have validated the online estimation for the rotor speed of an induction motor operating in an indirect rotor field orientated control (IRFOC) system based on Luenberger state observer (LSO). The complexity of the algorithm, however, is reduced by using analytical relations to obtain directly the Luenberger state observer (LSO) gain matrix L as function of the electrical velocity ω_r and the proportional constant $k_p \succ 1$. The proposed scheme is validated through simulation and experimental results. All experimental results confirm the good dynamic performances of the developed drive systems and show the validity of the proposed method.

NOMENCLATURE

v_{ds}, v_{qs}	: d, q-axis stator voltage components;
i_{ds}, i_{qs}	: d, q-axis stator current components;
Φ_{ds}, Φ_{qs}	: d, q-axis stator flux components;
R_s, R_r	: stator and rotor winding resistance;
L_s, L_r	: stator and rotor winding resistance;
M	: stator and rotor self-inductance;
n_p	: number of pole pairs;
$p \triangleq d/dt$	: differential operator;
ω_s, ω_r	: synchronous and rotor angular speed;
ω_{sl}	: slip angular speed $\omega_{sl} = \omega_s - \omega_r$;
T_e, T_l	: electromagnetic and load torque;
J	: moment of inertia;
f	: friction constant;
τ_s, τ_r	: stator and rotor time constant;
$k_{\omega i}$	: integral gain of the IP speed controller;
$k_{\omega p}$	: proportional gain of the IP speed controller;
$k_{I\hat{\omega}_r}$	: integral gain of the PI speed observer;
$k_{P\hat{\omega}_r}$	: proportional gain of the PI speed observer;
k_{ii}	: integral gain of the PI current controller;
k_{ip}	: proportional gain of the PI current controller;
σ	: total leakage constant;
^, *	: estimated and reference value;

APPENNDIX

List of motor specification and parameters 220/380V, 3KW, 4 poles, 1430 rpm
$R_s = 2.3\Omega$, $R_r = 1.83\Omega$, $L_s = 0.261H$, $L_r = 0.261H$, $M = 0.245H$,
$f = 0.002 Nm.s.rad^{-1}$ and $J = 0.03 Kg.m^2$

REFERENCES

[1] J. Jung, K. Nam, A dynamic decoupling control scheme for high speed operation of induction motor, *IEEE Transaction on Industry Applications*, vol. 30, 1994, pp. 1219-1224.

[2] F. J. Lin, R. J. Wai, C. H. Lin, and D. C. Liu, Decoupling stator-flux oriented induction motor drive with fuzzy neural network uncertainly observer, *IEEE Transaction on Industrial Electronics*, vol. 47, n. 2, 2000, pp. 356-367.

[3] S. Suwankawin and S. Sangwongwanich, A speed sensorless IM drive with decoupling control and stability analysis of speed estimation, *IEEE Transaction on Industrial Electronics*, vol. 49, n. 2, 2002, pp. 444-455.

[4] Y. Agrebi, M. Triki, Y. Koubaa, M. Boussak, Rotor speed estimation for indirect stator flux oriented induction motor drive based on MRAS Scheme, *Journal of Electrical Systems*, vol. 3, 2007, pp. 131–143.

[5] S. Maiti, C. Chakraborty, Y. Hori, and M. C. Ta, Model reference adaptive controller-based rotor resistance and speed estimation techniques for vector controlled induction motor drive utilizing reactive power, *IEEE Transaction on Industrial Electronics*, vol. 55, n. 2, 2008, pp. 594-601.

[6] Y. Koubaa, M. Boussak, Rotor resistance tuning for indirect stator flux oriented induction motor drive based on MRAS scheme, *Revue European Transactions on Electrical Power*, vol. 15, n. 6, 2005, pp. 557-570.

[7] Y. Agerbi, Y. Koubaa and M. Boussak, Online Rotor Resistance Estimation Using the Model Reference Adaptive System of Induction Motor, *I-manager's Journal on Electrical Engineering*, vol. 3, n. 3, 2010, pp. 1–10.

[8] M. Barut, S. Bogosyan, and M. Gokasan, Experimental evaluation of braided EKF for sensorless control of induction motors, *IEEE Transaction on Industrial Electronics*, vol. 55, n. 2, 2008, pp. 620-632.

[9] K. L. Shi, Y. K. Wong, and S. L. Ho, Speed estimation of an induction motor drive using an optimized extended Kalman filter, *IEEE Transaction on Industrial Electronics*, vol. 49, n. 1, 2002, pp. 124-133.

[10] Lu Qiang, Shen Chuan-wen, Ji Xiao-long, and Meng Yong-qing, A novel sliding-mode observer for speed-sensorless induction motors, *Proceedings of the CSEE*, vol. 26, 2006, pp. 164-168.

[11] A. B. Proca and A. Keyhani, Sliding-mode flux observer with online rotor parameter estimation for induction motors, *IEEE Transaction on Power Electronics*, vol. 54, n. 2, 2007, pp. 716-723

[12] Tae-Sung Kwon, Myoung-Ho Shin and Dong-Seok Hyun, Speed sensorless stator flux-oriented control of induction motor in the field weakening region using luenberger observer, *IEEE Transaction on Power Electronics*, vol. 20, n. 4, 2005, pp. 864-869.

[13] L. Jingchuan, L. Xu, Z. Zhang, An adaptive sliding-mode observer for induction motor sensorless speed control, *IEEE Transaction on Industrial Electronics*, vol. 46, n. 1, 1999, pp. 100-110.

[14] J. Maes and J. A. Melkebeek, Speed-Sensorless Direct Torque Control of Induction Motors Using an Adaptive Flux Observer, *IEEE Transaction on Industry Applications*, vol. 36, n. 3, 2000, pp. 778-785.

[15] H. Rehman, R. Dhaouadi, A fuzzy learning-Sliding mode controller for direct field-oriented induction machines, *Neurocomputing*, vol. 71, 2008, pp. 2693-2701.

[16] B. Karanayil, M. F. Rahman, and C. Grantham, Online stator and rotor resistance estimation scheme using artificial neural networks for vector controlled speed sensorless induction motor drive, *IEEE Transaction on Industrial Electronics*, vol. 54, n. 1, 2007, pp. 167-176.

[17] S. H. Kim, T. S. Park, and G. T. Park, Speed sensorless vector control of an induction motor using neural network estimation, *IEEE Transaction on Industrial Electronics*, vol. 48, n. 3, 2001, pp. 609-614.

[18] M. Boussak, K. Jarray, A High-Performance Sensorless Indirect Stator Flux Orientation of Induction Motor Drive, *IEEE Transaction on Industrial Electronics*, vol. 53, n. 1, 2006, pp. 41-49.